Johannes Taubert and Thomas Brüser*

Twin-arginine translocation-arresting protein regions contact TatA and TatB

Abstract: Tat systems translocate folded proteins across biological membranes of prokaryotes and plant plastids. TatBC complexes recognize N-terminal Tat signal peptides that contain a sequence motif with two conserved arginines (RR-motif), and transport takes place after a recruitment of TatA. Unfolded Tat substrate domains lower translocation efficiency and too long linkers lead to translocation arrest. To identify the components that interact with transported proteins during their passage through the translocon, we used a Tat substrate that arrests translocation at a long unfolded linker region, and we chose *in vivo* site-directed photo cross-linking to specifically detect the interactions of this linker region. For comparison, we included the interactions of the signal peptide and of the folded domain at the C-terminus of this construct. The data show that the linker contacts only two, structurally similar Tat components, namely TatA and TatB. These contacts depend on the recognition of the Tat-specific signal peptide. Only when membrane translocation of the globular domain was allowed – i.e., in the absence of the linker – we observed the same TatAB-contacts also to the globular domain. The data thus suggest that mature protein domains are translocated through a TatAB environment.

Keywords: membrane proteins; protein transport; protein-protein interactions; Tat system; twin-arginine translocation.

DOI 10.1515/hsz-2014-0170
Received March 17, 2014; accepted June 10, 2014

Introduction

The transport of folded proteins across biological membranes can be necessary, e.g., in cases when proteins have to assemble cofactors or when protein folding cannot be efficiently prevented before transport. In prokaryotes and plant plastids, the twin-arginine translocation (Tat) pathway serves this purpose (Palmer and Berks, 2012). Surprisingly, only a membrane energetization and minimally only two unique membrane proteins are required for function (Goosens et al., 2014). These membrane proteins – termed TatA and TatC – are small proteins with usually lower than 10 or 30 kDa molecular mass, respectively. In plants as well as in the model bacterium *Escherichia coli*, a third component – TatB – exists, which resembles TatA but has a higher affinity to TatC (Sargent et al., 1999; Bolhuis et al., 2001). Tat proteins can oligomerize to form large associations or complexes (Oates et al., 2005; Richter and Brüser, 2005). A series of translocation events mediates the passage of the protein substrate through the membrane (Hou and Brüser, 2011). It is clear that TatBC complexes recognize N-terminal signal peptides of Tat substrates by their eponymous 'twin-arginine' (RR-) motif, which includes two adjacent arginines in a conserved environment (Cline and Mori, 2001). After this recognition, a number of TatA protomers are recruited and currently believed to form a punctually destabilized membrane in direct vicinity to TatBC (Brüser and Sanders, 2003; Dabney-Smith et al., 2006; Rodriguez et al., 2013). Then the folded 'mature domain' of the Tat substrate is somehow channeled through this TatA-containing association. This step may be triggered by TatBC-mediated signal peptide pulling (Brüser and Sanders, 2003; Rodriguez et al., 2013). In agreement with this hypothesis, TatC can remain bound to the signal peptide throughout translocation and it has been shown to have a signal peptide insertase activity (Gerard and Cline, 2006; Fröbel et al., 2012).

So far, no late translocation intermediate could be identified where a substrate was trapped in its natural environment during the membrane passage. To artificially generate such trapped substrates, long unfolded peptides were inserted in between Tat signal peptides and folded globular domains (Cline and McCaffery, 2007; Lindenstrauß and Brüser, 2009). In studies on the plant TatABC system, the trapped substrates appeared to be immediately released from the translocon, as (i) no Tat components could be detected in the environment of such

***Corresponding author: Thomas Brüser,** Institut für Mikrobiologie, Leibniz Universität Hannover, Schneiderberg 50, 30167 Hannover, Germany, Phone: +49 511 762 5945, Fax: +49 511 762 5287, e-mail: brueser@ifmb.uni-hannover.de
Johannes Taubert: Institut für Mikrobiologie, Leibniz Universität Hannover, Schneiderberg 50, 30167 Hannover, Germany

constructs and as (ii) this translocation arrest did not negatively affect subsequent translocation of other Tat substrates *in vitro* (Cline and McCaffery, 2007). Translocation of trapped substrates is thus aborted. A cross-linking with actively translocating systems should allow for the detection of the specific environment of the unfolded translocation-arresting regions during membrane-passage or thereafter. A site-specific cross-linking that selectively addresses the environment of the unfolded translocation-arresting protein domain has not been carried out so far. In contrast, Tat cross-links to folded mature domains of translocation-compatible Tat substrates have been intensively studied and a translocation through a TatA environment has been proposed (Brüser and Sanders, 2003; Maurer et al., 2010; Aldridge et al., 2012; Pal et al., 2013; Rodriguez et al., 2013).

Using *in vivo* site directed cross-linking, we addressed the question which Tat system components are contacted by translocation-arresting unfolded regions of mature domains of Tat signal peptide-containing proteins. The data show that mature domains of Tat substrates contact TatA and especially TatB components, which likely surround substrates when they traverse the membrane.

Results

In *E. coli*, the Tat machinery is used for translocation of folded proteins across the cytoplasmic membrane. In studies on plant and bacterial Tat systems, long unfolded linker peptides that are inserted in between Tat signal peptides and globularly folded domains have been shown to abort Tat translocation (Cline and McCaffery, 2007; Lindenstrauß and Brüser, 2009). In the plant study, a $(Gly_4Ser)_{15}$-linker was used to abort translocation and no Tat components could be detected that contacted the mature domain of this construct, suggesting a rapid dissociation from translocon components after translocation abortion (Cline and McCaffery, 2007). In case of the bacterial study, the natively unfolded FG-repeats of yeast nuclear pore protein Nsp1p have been used as linkers (Lindenstrauß and Brüser, 2009). Contacts of these constructs to Tat components have not been examined at that time.

For that purpose, we introduced the artificial photoactivatable cross-linker amino acid *p*-benzoylphenylalanine (*p*Bpa) *in vivo* into selected positions of the translocation-aborting Tat substrate. We used the RR-(FG10)-HiPIP substrate that contains a 205-residue linker of ten natively unfolded FG-repeats in tandem (FG10) sandwiched in between the Tat-specific signal peptide and the tightly folded mature domain of the model Tat substrate HiPIP (Figure 1A). RR-(FG10)-HiPIP has previously been shown to abort Tat transport (Lindenstrauß and Brüser, 2009). Similar to the $(Gly_4Ser)_{15}$-linker constructs that had been used in studies on the plant Tat system, over-production of RR-(FG10)-HiPIP does not compromise Tat transport of other substrates, which is suggestive of a release of arrested substrates from the translocon. For example, the Tat system can still translocate the natural Tat substrate TorA or the amidases AmiA and AmiC under these conditions, which ensures proper cell separation after cell division (Figure 1BC). Without Tat transport of these amidases, cell chains are formed [Figure 1C, left, and (Ize et al., 2003)]. For ribosomal incorporation of *p*Bpa at desired positions, we used an orthogonal suppressor tRNA/aminoacyl tRNA synthetase pair that was developed by the group of Peter G. Schultz to specifically translate TAG stop codons into *p*Bpa (Chin et al., 2002; Ryu and Schultz, 2006; Young et al., 2010). *p*Bpa was thereby placed at position A13 and

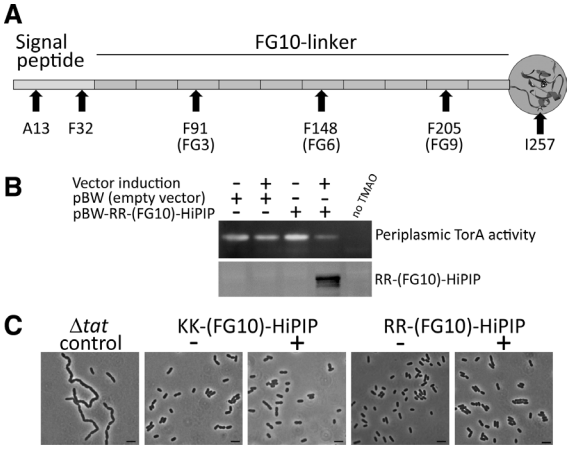

Figure 1 The Tat-system is not blocked by translocation-arresting Tat-Substrates.
(A) Scheme of the studied linker-containing Tat substrate RR-(FG10)-HiPIP and positions of the introduced cross-linking amino acids. The globular HiPIP structure was generated using protein data bank (PDB) 1hip coordinates and the Swiss-PDB-viewer (Guex and Peitsch, 1997). (B) TorA can be translocated when RR-(FG10)-HiPIP is produced. Strains carrying the rhamnose-inducible pBW-RR-(FG10)-HiPIP vector or the corresponding empty vector were grown with or without induction, and TMAO-reductase activity was detected in the corresponding periplasmic fractions. In one culture (last lane '-TMAO'), TMAO was omitted to confirm the TMAO-dependence of the band. The lower blot shows the production of RR-(FG10)-HiPIP in cell extracts of the cultures. (C) Microscopic analysis of the chain formation phenotype in strains MC4100 pRK-*tatABC*/pEvol*p*BpF/pBW-FG10-hip-F148*p*Bpa (RR/KK variants) under induced (+) and non-induced (-) conditions. The Tat-deficient strain DADE (Δ*tat*) served as a positive control for the chain formation phenotype (left panel). Recombinantly produced RR-(FG10)-HiPIP did not interfere with cell division and thus did not block Tat transport.

F32 of the signal peptide, at the F position of FG repeats 3, 6, and 9 (F91, F148, F205), and at position I257, which is an exposed residue on the surface of the folded HiPIP domain (Figure 1A). Cross-links were induced by UV-illumination and detected after affinity enrichment by Western blotting. To address RR-motif dependence and thus a dependence of the cross-links from TatBC-recognition, we also examined RR>KK variants in which the two conserved arginines of the twin-arginine motif were charge-conservatively exchanged by lysines. This exchange strongly reduces the affinity to TatBC and thereby selectively inhibits or abolishes Tat transport (Halbig et al., 1999; Stanley et al., 2000; Cline and Mori, 2001; Alami et al., 2003).

The cross-links to signal peptide positions are shown in Figure 2. For the detection of transient Tat contacts by cross-links that are generated with actively transporting systems *in vivo* in the presence of high levels of interacting chaperones etc., a ~200-fold enrichment of the substrate by affinity purification and TCA precipitation was required. For comparison of cross-link efficiencies, the non-enriched solubilized membrane fraction was always loaded on the same gel (left lane). Up to ~3% of the Tat components were cross-linked, detectable as shifted bands in elution fractions 2 and 3 of the affinity chromatographies. The intensities of the specific signals were comparable to *in vitro* studies that could use selectively radiolabeled substrates to increase the assay sensitivity (Alami et al., 2003). In agreement with these studies, TatB and TatC cross-links to the signal peptide were strongly enhanced by the intact RR-motif, which indicates the recognition of the RR-motif by TatBC complexes (Figure 2A). These cross-links were most prominent at position F32. Residual cross-linking to KK-variants is expected as physiological studies indicate low-efficient Tat-dependent translocation of RR>KK mutated Tat substrates (Ize et al., 2002; Kreutzenbeck et al., 2007). The contacts to TatBC are in line with the view that a large region of the signal peptide is bound by actively translocating TatBC complexes. TatA cross-links to the signal peptide were less influenced by the twin-arginine motif.

To examine the possible PMF-dependence of the signal peptide Tat interactions, we carried out the cross-linking experiments in the presence of 100 µM carbonyl cyanide m-chlorophenyl hydrazone (CCCP), a protonophor commonly used to abolish the PMF (Alami et al., 2003; Berthelmann et al., 2008). While the interactions to position A13 were not compromised under these conditions, we detected a very strong reduction of TatABC cross-links to *p*Bpa at position F32, indicating that this region of the signal peptide requires the PMF to tightly associate with TatABC (Figure 2B).

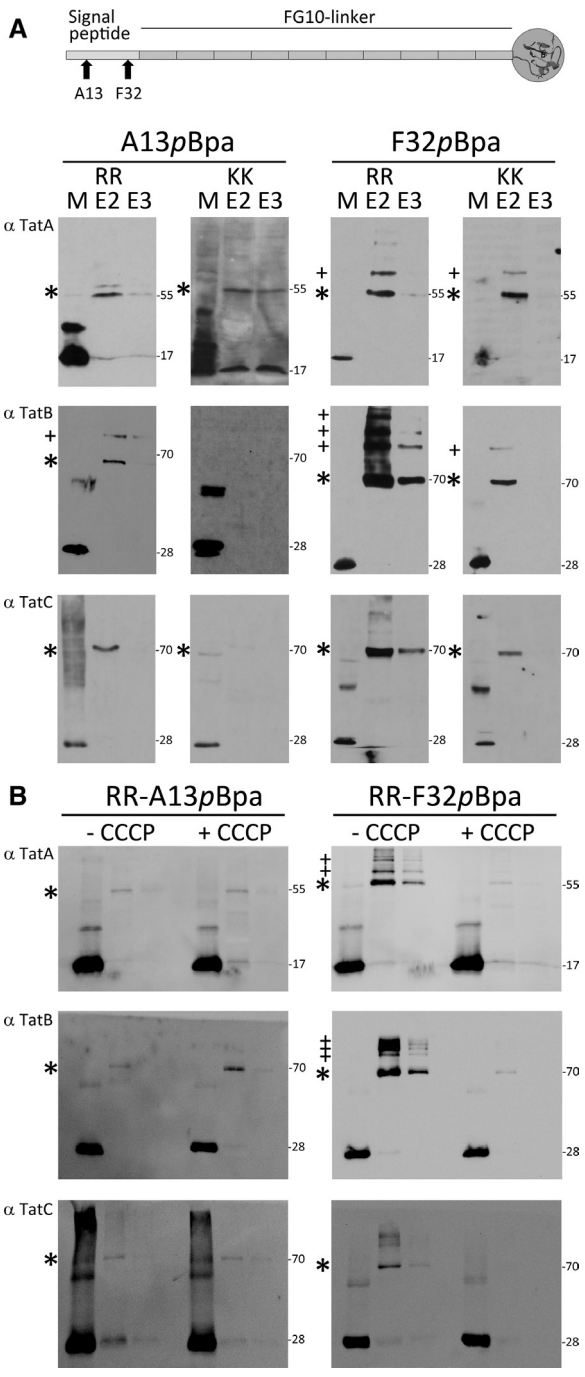

Figure 2 The signal peptide is in direct environment to TatABC. (A) *In vivo* site directed photo cross-linking analyses of RR/KK signal peptide interactions with TatABC. Positions of *p*Bpa are indicated. Cross-links to the Tat components were detected in elution fractions 2 and 3 after Western blot analyses using indicated Tat specific antibodies. Note that twin-lysine (KK) variants showed weaker cross-links to TatB and TatC, whereas TatA cross-links were less influenced. (B) Analysis of the effect of 100 µM CCCP on *in vivo* cross-linking to TatABC. Experiments were carried out as described under (A), using the indicated substrates. Molecular weight standards are indicated at the right. *, single cross-links; +, additional cross-links; M, membrane fraction; E, elution fraction.

The cross-links to the linker region readily revealed that the linker is in close proximity to TatA and TatB (Figure 3A). Especially the TatB cross-links were pronounced. Double bands indicated either processing (the tagged C-terminus of the substrate must have been intact for the affinity purification) or heterogeneous migration behavior of the cross-linked products (see Discussion). In case of TatA cross-links, we repeatedly detected smaller degradation bands that may reflect some proteolysis after affinity enrichment. The RR>KK mutation depleted all cross-links with the linker region (Figure 3B), indicating that TatA and TatB contact the linker region after TatBC complex recognition, which can be any step from binding to release of the transported substrate. In the *in vivo* experimental setup, in which CCCP affects the systems' energetization (ATP levels), the formation of the cross-links did not depend on the PMF (Figure 3B, right blots). Due to the requirement of substrate production prior to CCCP addition in the *in vivo* assay system, the cross-links cannot differentiate between already membrane-inserted linker-substrates or substrates that are bound at the translocon (see Discussion). A selective stabilization of the largest TatB-cross-link by CCCP is suggestive for inhibited proteolysis of already membrane-inserted linker-substrate in de-energized cells.

We finally assessed the Tat component contacts of the globular HiPIP mature domain and chose a single hydrophobic residue on the surface of HiPIP for substitution by *p*Bpa (I257; corresponds to I52 in natural HiPIP precursor, Figure 4). To examine the effect of the linker on these interactions, we included also the translocation competent natural HiPIP in these analyses. Before cross-linking was carried out, we ensured that *p*Bpa does not interfere with cofactor assembly and stability of HiPIP. Like natural HiPIP, *p*Bpa-containing HiPIP was highly stable so that the $[4Fe\text{-}4S]^{2+/3+}$ cofactor remained bound even in ESI-mass-spectrometry analyses (Figure 4B). The purified HiPIP showed the correct precursor mass (the N-terminal methionine removed) as well as the mass of correctly processed translocated HiPIP. The UV-vis spectrum of the *p*Bpa-containing variant was identical to the characteristic spectrum of natural HiPIP with the exception of additional UV-absorption that was due to the single incorporated aromatic *p*Bpa (Figure 4C). The selected residue was therefore perfectly suited to perform cross-linking at the surface of the globular HiPIP domain (Figure 4D).

The linker-free natural HiPIP showed strong contacts to TatB and TatA. Additional TatB signals at higher molecular weight suggest that more than one substrate can cross-link to individual TatB protomers. The TatA

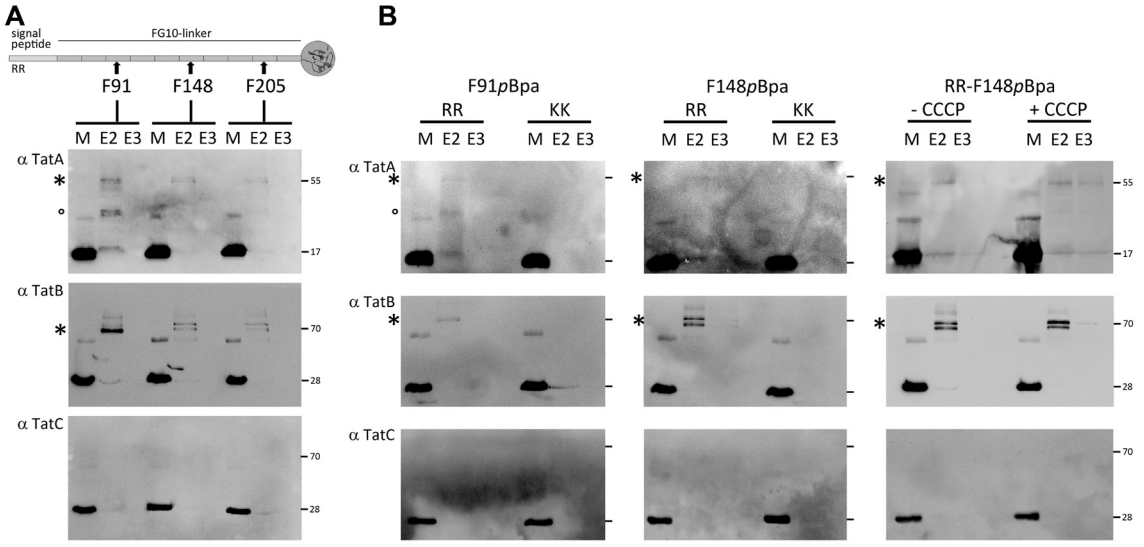

Figure 3 The linker region shows pronounced TatB contacts and weak TatA contacts.
In vivo site directed photo cross-linking analyses of linker interactions with TatABC. (A) Scheme of the RR-(FG10)-HiPIP fusion construct with indicated *p*Bpa cross-linker positions and blots of the corresponding cross-link-detections, using indicated Tat specific antibodies. (B) Strict RR-dependence and PMF-independence of the cross-links to TatA and TatB. Left and middle blots: Direct comparison of RR-(FG10)-HiPIP and KK-(FG10)-HiPIP cross-links at indicated positions. Right blots: Dissipation of the PMF by CCCP does not reduce the cross-links, as shown with position F148*p*Bpa. See Figure 2 for more details.

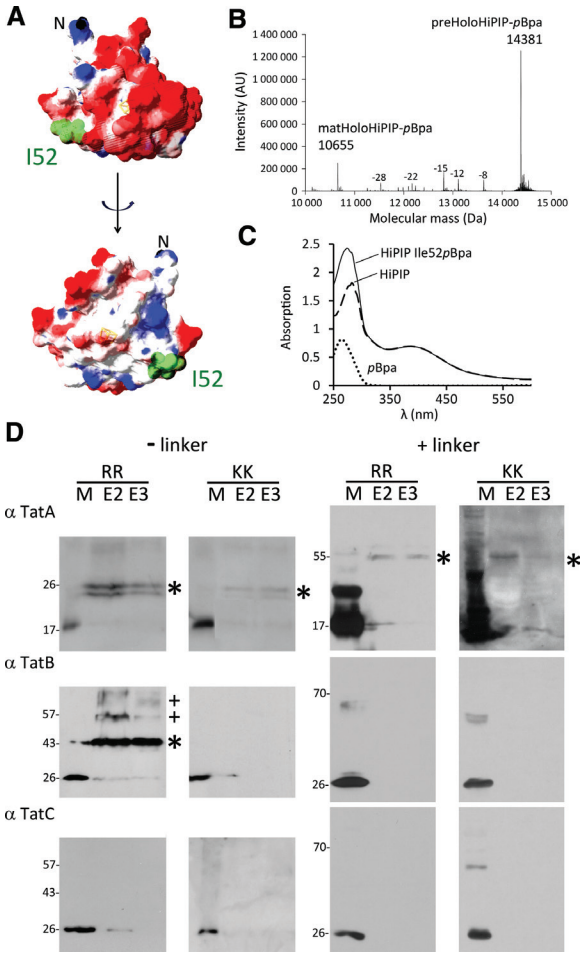

Figure 4 TatB cross-links to the folded globular domain depend on transport compatibility.
(A) Position of I52 (green) on the surface of the HiPIP mature domain. The model was generated by Swiss PDB-viewer (Guex and Peitsch, 1997) using PDB-1hip (Carter et al., 1974). Surface colours indicate the electrostatic potential (negative/red to positive/blue). (B) ESI-MS spectrum of HiPIP-I52*p*Bpa after purification from the soluble fraction. Mass peaks correspond to precursor or mature HiPIP with incorporated $[4Fe\text{-}4S]^{2+/3+}$ cluster and *p*Bpa at position I52 (preHoloHiPIP-*p*Bpa, matHoloHiPIP-*p*Bpa). Low-abundant of degradation signals all correspond to cleavages in the signal peptide region (some positions relative to full-length are indicated). (C) UV-Vis spectra of HiPIP (dashed line), HiPIP-I52*p*Bpa (continuous line) and *p*Bpa (dotted line) alone. The iron-sulfur cofactor absorbance around 390 nm indicates cofactor content of both proteins. The additional absorbance in the UV region of the HiPIP variant is due to *p*Bpa absorbance at 265 nm (Kauer et al., 1986). (D) *In vivo* photo cross-linking analyses of HiPIP-I52*p*Bpa (left panels, – linker) and the linker variant HiPIP-(FG10)-I257*p*Bpa (right panels, + linker) showing interactions of the folded HiPIP domain to the Tat components. RR>KK mutated variants are included to examine RR-dependence of the cross-links. Molecular weight standards are indicated at the left. See Figure 2 for more details.

cross-links were significantly enhanced by the recognition of the RR-motif, and TatB cross-link signals were completely RR-dependent, indicating that TatAB contacts require the RR-motif recognition by TatBC. The TatB cross-links were well-resolved bands that did not indicate any processing of the cross-linked protein. The analyses of the linker-containing construct revealed that TatB contacts to the globular domain were completely abolished by the linker. Weak, largely RR-independent TatA contacts were still detectable. Together, these data suggest that the folded mature domain only contacts TatB when it can be translocated, which implies that TatB co-operates with TatA at this stage of translocation.

Discussion

Without translocation arrest, membrane-translocated proteins are only very transiently in the environment of the translocon components. To analyze the translocon and substrate interactions during membrane passage, incompletely translocated stages are often generated artificially, and the accumulating translocation intermediates can then be used for biochemical or biophysical analyses [e.g., (Hou et al., 2012; Gogala et al., 2014; Park et al., 2014)]. In case of the Tat system that transports fully folded proteins, incomplete folding can result in translocation arrest that can be harmful to the cells (Richter and Brüser, 2005). Such a translocation arrest can be artificially induced by long unfolded linker peptides that are fused to folded globular protein domains (Cline and McCaffery, 2007; Lindenstrauß and Brüser, 2009). However, the Tat translocon is not completely blocked by such translocation arrests and results in translocation abortion that allows for new translocation cycles with newly recruited substrates (Cline and McCaffery, 2007) (Figure 1B). The Tat system thus seems to have a way to liberate arrested proteins. It is very likely that this mechanism relates to the natural recruitment and release of TatA in the translocation cycle (Mori and Cline, 2002), which can function as an intrinsic rescue pathway when the translocon is jammed. While Tat components did not interact with $(Gly_4Ser)_{15}$ linker-containing translocation-aborted Tat substrates (Cline and McCaffery, 2007), our detection of TatA and TatB interactions to the FG10-linker points to more persistent Tat interactions of this very distinct linker: The FG10-repeat is highly charged (30% K/D/E), rich in flexible residues (41% G/S/T/A), and contains two single hydrophobic residues (L/F) in each repeat. It is likely that dissociation rates from Tat components depend on structural properties, and the $(Gly_4Ser)_{15}$ linker most likely cannot mediate any significant interaction with the system.

The linker contacts to TatA and TatB as well as the signal peptide contacts to TatB and TatC were clearly RR-dependent (Figures 2 and 3). RR-dependence indicates physiologically relevant contacts that are mediated by the interaction of the RR-motif with the TatBC complex (Kreutzenbeck et al., 2007; Lausberg et al., 2012). TatA contacts to the signal peptide and to the folded mature domain showed less or no RR-dependence, which might point to an autonomous TatA interaction *in vivo*, such as described in Tat systems of other organisms (Pop et al., 2003; De Keersmaeker et al., 2007). While the RR-dependent signal peptide contacts obviously correspond to the substrate recognition step, the RR-dependent linker cross-links can be also due to any contacts of later translocation stages, such as the membrane passage or the substrate release. In many cases, we observed split signals, two closely migrating bands that may represent partial proteolytic degradation or simply differences in migration behavior depending on the cross-link position. In case of the TatA cross-links, the latter explanations are likely, as even the cross-link to linker-free HiPIP gave a doublet signal (Figure 4). With TatB cross-links, such doublet signals may represent partial N-terminal proteolysis, as these doublets were only seen in linker constructs that in principle can allow for the dissociation of signal peptides from translocons that are cross-linked to the substrate at linker positions far away from the signal peptide (Figure 3). A dissociation of the signal peptide from the Tat system has been shown to be a prerequisite for signal peptide cleavage and likely is required for any N-terminal proteolysis (Gerard and Cline, 2006; Frielingsdorf and Klösgen, 2007). It should be noted that the cross-links of the linker region were not enhanced in comparison to cross-links to the mature domain of linker-less HiPIP (Figures 3 and 4), which fully agrees with the view that the linker results in translocation abortion and dissociation of the translocon components (Cline and McCaffery, 2007).

The TatA data agree with the currently accepted view that translocation occurs through a TatA association in close contact to TatBC complexes (Brüser and Sanders, 2003; Aldridge et al., 2012; Pal et al., 2013; Rodriguez et al., 2013). Only in the linker region, TatA cross-links are clearly RR-dependent (Figure 3), which adds further evidence for a TatA environment that is generated during transport whereas TatA appears to interact with the signal peptide and the mature domain of HiPIP also RR-independently (Figures 2 and 4). However, our cross-links show TatB contacts that are at least as strong as TatA contacts, suggesting that TatB can co-operate with TatA in this step. Although it cannot be excluded that flexible linkers contact C-terminal regions of TatB in nearby TatBC complexes, it has to be recognized that similar TatC contacts were not observed. Moreover, *in vivo* cross-linking was carried out with actively translocating translocons over a time scale of 30 min, and the method should thus detect any contacts throughout the translocation cycle. The fact that the TatAB cross-links could also be detected with the globular domain if only this domain was allowed to traverse the membrane – i.e., in the absence of the linker – strongly suggests that translocation takes place through a TatAB environment. The linker cross-links were independent from the PMF, which discloses limitations of the *in vivo* test system that cannot differentiate whether detected contacts correspond to substrate that accumulated in membranes prior to CCCP-addition or to bound substrate prior to PMF-dependent steps (Figure 3). The latter scenario is highly unlikely, since we cross-linked in actively transporting cells and since the linker alone is known to be Tat-dependently translocated (Richter et al., 2007; Lindenstrauß and Brüser, 2009). Support for the accumulation-scenario comes also from the observation that the upper band of the double band was reproducibly enhanced by CCCP-treatment, implying CCCP-effects of ATP-dependent proteolysis of membrane-accumulated linker-substrates. Moreover, the F32 position of the signal peptide strongly contacted PMF-dependently TatABC, reflecting an active movement of the end of the signal peptide h-region into an environment tightly associated with TatABC (Figure 2). Obviously, the signal peptide of the linker-construct is transported, resulting in some membrane-inserted species. The proposed signal peptide-binding groove of TatC spans the membrane (Rollauer et al., 2012; Ramasamy et al., 2013) and therefore the complete h-region of the signal peptide should interact with the translocon at least in actively translocating systems. Our cross-linking data now for the first time support this experimentally in a bacterial system and clearly differentiate between a PMF-independent binding of the RR motif to TatABC and a PMF-dependent signal peptide movement, most likely into the almost trans-membrane positioned binding pocket. This is in full agreement with studies on the plant system that demonstrated a PMF-dependent deeper binding of signal peptides into TatBC complexes (Gerard and Cline, 2007). In that study, the complete signal peptide insertion was inhibited by TatA antibody-treatment, whereas in our *in vivo* system the signal peptide will be membrane-inserted due to the presence of all active components.

A closer look at the TatB component renders the above described 'TatA/TatB-co-operation scenario' very likely: TatB belongs to the same protein family and apparently originates from a gene duplication of TatA (Yen

et al., 2002). In early studies that used a very sensitive physiological translocation assay to examine the effect of *tat* gene deletions on Tat transport, a residual Tat transport by TatBC systems in the complete absence of TatA has been observed (Ize et al., 2002). Albeit the used assay was extremely sensitive, these studies showed that TatB can in principle complement (with very low efficiency) for the function of TatA. The membrane permeabilization is currently believed to mainly relate to the unusual N-terminal TatA membrane anchor with a short stretch of only 13 consecutive hydrophobic residues that weakens the membrane when many TatA protomers cluster (Rodriguez et al., 2013). However, TatB has exactly the same unusual membrane anchor characteristics and there is no reason to believe that this highly conserved TatB feature is coincidental. The differentiation between TatA and TatB is quite artificial as there is no clear differential functionality attributed to either component yet. TatB can be regarded as a TatA that interacts more strongly with TatC at the site of translocation (Hou and Brüser, 2011). The generally accepted 1:1 ratio of TatB:TatC (Bolhuis et al., 2001), which is seen in the detergent-stable core complex, is significantly altered to up to 4:1 already by single point mutations (Barrett et al., 2005) and it is thus possible that additional TatB is present at lateral positions that are currently reserved for TatA. Trans-membrane-domains of TatA and TatB have been reported to co-operate (Barrett and Robinson, 2005), single amino acid exchanges in TatA have been shown to make TatB dispensable (Blaudeck et al., 2005), TatAB complexes have been described (Oates et al., 2005), and TatB is produced in a two-fold excess over TatC in *E. coli* (Jack et al., 2001). Moreover, the TatA contents can be very low in plant species (Jakob et al., 2009), and TatA and TatB functions in naturally occurring TatAC systems are carried out by a single protein that is then termed TatA (Goosens et al., 2013). Such bifunctional TatA can even complement *tatA* and *tatB* mutations in *E. coli* (Barnett et al., 2008). All these observations question the rather arbitrary distinction of TatA and TatB functions in active translocons and are suggestive for highly similar substrate interactions of the TatA and TatB components, which most likely differ only in their affinities to TatC.

Our data would agree with the scenario that TatB and TatA co-operate to form the environment of the translocated protein, and the unusual short hydrophobic stretches in the membrane anchors of both components are likely to play a key role in the process of assembly and membrane destabilization. We cannot tell whether the detected TatB originated from TatBC complexes or from TatAB complexes, but at the active TatABC translocon these differentiations may become meaningless anyway.

Materials and methods

Strains and growth conditions

Escherichia coli strain MC4100 ara^R (Casadaban, 1976) was used for *in vivo* photo cross-linking, and *E. coli* XL1-Blue Mrf'Kan (Stratagene) was employed for cloning. Strains were grown aerobically at 37°C on LB medium (1% tryptone, 1% NaCl, 0.5% yeast extract) in the presence of appropriate antibiotics (100 μg/ml ampicillin, 25 μg/ml chloramphenicol, 12.5 μg/ml tetracycline). For anaerobic growth, LB medium was supplemented with 0.5% glycerol and 0.4% nitrate. TMAO reductase (TorA) production was induced by addition of 1.1% TMAO. When indicated, proton motif force (PMF) was abolished by addition of 100 μM carbonyl cyanide 3-chlorophenylhydrazone (CCCP).

Plasmids and genetic methods

The plasmid pEvol*p*BpF that encodes an orthogonal *p*Bpa-specific suppressor tRNA/aminoacyl tRNA synthetase pair was used for incorporation of *p*Bpa at introduced amber stop codons (Young et al., 2010). The *tatABC* genes were constitutively ~15-fold expressed by the plasmid pRK-*tatABC* (Brüser et al., 2003). Tat signal peptide-linker-HiPIP fusion proteins containing the HiPIP signal peptide fused to 10 natively unfolded FG repeats and the C-terminally his_6-tagged mature domain of HiPIP were produced using pBW-FG10-hip (Richter et al., 2007). Amber stop mutations were inserted by QuikChange™ mutagenesis with pBW-R10-hip and pBW-R10-hip-KK as template in combination of forward primers and complementary reverse primers. The position 13 encoding for alanine and position 32 encoding for phenylalanine in the HiPIP signal peptide was exchanged to amber stop codon using forward primers hip-RR-A13*p*Bpa-F (5′-AGC AAG AGC CGT CGT GAC TAG GTC AAA GTG ATG CTG-3), hip-KK-A13*p*Bpa-F (5′-AGC AAG AGC AAG AAA GAC TAG GTC AAA GTG ATG CTG-3′) and hip-F32*p*Bpa-F (5′-ATC AAC CTG GTC GGT TAG GGC ACC GCC CGT GCC-3′). The phenylalanine codon of the FG repeat 3, 6 and 9 was mutated using forward primers FG3*p*Bpa-F (5′-AAG CCT GCC TTC TCA TAG GGT GCT AAG CCA GAA-3′), FG6*p*Bpa-F (5′-AAG CCG GCA TTC TCT TAG GGA GCA AAG TCT GAT G-3′) and FG9*p*Bpa-F (5′-AAA CCA GCT TTC TCA TAG GGT GCC AAA TCA AAT G-3′), respectively. For constitutive HiPIP production, the plasmids pEXH5tac-H6 and pEXH5tac-KK-H6 were used. A C-terminal His_6-tag-coding sequence was fused to the *hip* gene by cloning the corresponding PvuI fragment from pEXH7 into the PvuI-digested pEXH5tac/pEXH5tac-KK (Brüser et al., 1998). Position I52 in the mature domain of HiPIP and the corresponding site in the linker construct (I257) were mutated to amber stop codons using the template pEXH5tac-H6/pEXH5tac-KK-H6, pBW-R10-hip (RR/KK) and the primer hip-I52*p*Bpa-F (5′-GAC GAT GCG ACC GCG TAG GCC CTC AAG TAC AAC-3′) in conjunction with the complementary reverse primer. All constructs were confirmed by DNA sequencing.

Biochemical methods

For incorporation of *p*Bpa at amber stop codon positions in strains carrying the pEvol*p*BpF system, 100 μM *p*Bpa were added simultaneously with 100 μM L-arabinose together with or without 6 mM L-rhamnose to growing cultures 3 h before UV cross-linking. *p*Bpa was activated by irradiation with UV light at 365 nm for 30 min

at ambient temperature. Membranes were prepared according to standard protocols (Brüser et al., 2003) and solubilized for 30 min in 20 mM Tris-HCl, pH 8.0, 3% SDS. The preparation was diluted with detergent-free buffer to 0.1% SDS, non-solubilized material was separated by ultracentrifugation (130 000×*g*, 30 min, 25°C), and the supernatant was used for affinity chromatography. Affinity purification was carried out as described elsewhere (Lindenstrauß and Brüser, 2009), but under denaturing conditions (0.1% SDS). Elution fractions 2 and 3 were 6-fold concentrated by trichloroacetic acid precipitation, resulting in a total enrichment of ~200-fold in the analyzed elution fractions. Nitrocellulose membranes were used for Western blotting and proteins were detected by the ECL system (GE Healthcare Europe, Freiburg, Germany) using antibodies directed against C-terminal peptides of TatA, TatB, TatC, or full-length HiPIP. For structural analysis of HiPIP variants, cells were harvested at $OD_{600\ nm}$=2.5. Protein was purified from the soluble fraction by Ni-NTA chromatography (Lindenstrauß and Brüser, 2009). Fractions containing the purified HiPIP were combined and dialyzed against 20 mM Tris-HCl, pH 9.0 and loaded on a DEAE-Sephacel (GE Healthcare Europe, Freiburg, Germany) column, equilibrated with the same buffer. Bound HiPIP was eluted by shift to pH 6.8 with 50 mM ammonium acetate. The eluted HiPIP-containing fractions were pooled and concentrated by ultrafiltration centrifugation (5 kDa cut off). Spectra were recorded on a UVICON 900 double beam spectrophotometer (Kontron Instruments, Neufahrn, Germany). Samples were analyzed by ESI-MS with the use of an LTQ-OrbitrapXL mass spectrometer (ThermoFisher Scientific, Bremen, Germany). Mass spectra of peptides were acquired offline by nanoESI (Proxeon, Odense, Denmark) in the positive ionization mode. The m/z range was 200–2000 and the resolving power was R=30 000 at m/z 400. Fragments induced by CID (collision-induced dissociation) were detected in the orbitrap mass analyzer. For microscopy, strains were cultivated to exponential growth phase under induced and non-induced conditions and visualized by differential interference contrast using Axio Imager.M2 and AxioCam Mrm digital camera (Zeiss, Jena, Germany). For preparation of periplasmic fractions by osmotic shock, cells from exponentially growing anaerobic cultures (50 ml) were harvested (4500×*g*, 4°C) and resuspended in 20 ml 20% sucrose/10 mM Tris-HCl pH 8.0/1 mM EDTA, incubated for 10 min at room temperature, and again sedimented. The supernatant-free cell pellet was resuspended in ice-cold 1 ml 5 mM $MgSO_4$ and incubated for 20 min on ice. Shocked cells were sedimented (9500×*g*, 4°C) and the periplasm (supernatant) was carefully collected. TorA activity was detected in native gels as described elsewhere (Silvestro et al., 1989).

Acknowledgments: We thank Peter G. Schultz (The Scripps Research Institute, La Jolla) for donation of the pEVOL system, and Andrea Sinz and Christian Ihling (University of Halle-Wittenberg) for mass spectrometry analysis. This work was funded by the Deutsche Forschungsgemeinschaft (GRK 1026: 'Conformational transitions during macromolecular interactions').

References

Alami, M., Lüke, I., Deitermann, S., Eisner, G., Koch, H.G., Brunner, J., and Müller, M. (2003). Differential interactions between a twin-arginine signal peptide and its translocase in *Escherichia coli*. Mol. Cell. *12*, 937–946.

Aldridge, C., Storm, A., Cline, K., and Dabney-Smith, C. (2012). The chloroplast twin arginine transport (Tat) component, Tha4, undergoes conformational changes leading to Tat protein transport. J. Biol. Chem. *287*, 34752–34763.

Barnett, J.P., Eijlander, R.T., Kuipers, O.P., and Robinson, C. (2008). A minimal Tat system from a gram-positive organism: a bifunctional TatA subunit participates in discrete TatAC and TatA complexes. J. Biol. Chem. *283*, 2534–2542.

Barrett, C.M. and Robinson, C. (2005). Evidence for interactions between domains of TatA and TatB from mutagenesis of the TatABC subunits of the twin-arginine translocase. FEBS J. *272*, 2261–2275.

Barrett, C.M., Mangels, D., and Robinson, C. (2005). Mutations in subunits of the *Escherichia coli* twin-arginine translocase block function via differing effects on translocation activity or Tat complex structure. J. Mol. Biol. *347*, 453–463.

Berthelmann, F., Mehner, D., Richter, S., Lindenstrauß, U., Lünsdorf, H., Hause, G., and Brüser, T. (2008). Recombinant expression of *tatABC* and *tatAC* results in the formation of interacting cytoplasmic TatA tubes in *Escherichia coli*. J. Biol. Chem. *283*, 25281–25289.

Blaudeck, N., Kreutzenbeck, P., Müller, M., Sprenger, G.A., and Freudl, R. (2005). Isolation and characterization of bifunctional *Escherichia coli* TatA mutant proteins that allow efficient Tat-dependent protein translocation in the absence of TatB. J. Biol. Chem. *280*, 3426–3432.

Bolhuis, A., Mathers, J.E., Thomas, J.D., Barrett, C.M., and Robinson, C. (2001). TatB and TatC form a functional and structural unit of the twin-arginine translocase from *Escherichia coli*. J. Biol. Chem. *276*, 20213–20219.

Brüser, T. and Sanders, C. (2003). An alternative model of the twin arginine translocation system. Microbiol. Res. *158*, 7–17.

Brüser, T., Deutzmann, R., and Dahl, C. (1998). Evidence against the double-arginine motif as the only determinant for protein translocation by a novel Sec-independent pathway in *Escherichia coli*. FEMS Microbiol. Lett. *164*, 329–336.

Brüser, T., Yano, T., Brune, D.C., and Daldal, F. (2003). Membrane targeting of a folded and cofactor-containing protein. Eur. J. Biochem. *270*, 1211–1221.

Carter, C.W. Jr., Kraut, J., Freer, S.T., Nguyen Huu, X., Alden, R.A., and Bartsch, R.G. (1974). Two-Angstrom crystal structure of oxidized *Chromatium* high potential iron protein. J. Biol. Chem. *249*, 4212–4225.

Casadaban, M.J. (1976). Transposition and fusion of the lac genes to selected promoters in *Escherichia coli* using bacteriophage lambda and Mu. J. Mol. Biol. *104*, 541–555.

Chin, J.W., Martin, A.B., King, D.S., Wang, L., and Schultz, P.G. (2002). Addition of a photocrosslinking amino acid to the genetic code of *Escherichia coli*. Proc. Natl. Acad. Sci. USA *99*, 11020–11024.

Cline, K. and McCaffery, M. (2007). Evidence for a dynamic and transient pathway through the TAT protein transport machinery. EMBO J. *26*, 3039–3049.

Cline, K. and Mori, H. (2001). Thylakoid ΔpH-dependent precursor proteins bind to a cpTatC-Hcf106 complex before Tha4-dependent transport. J. Cell Biol. *154*, 719–729.

Dabney-Smith, C., Mori, H., and Cline, K. (2006). Oligomers of Tha4 organize at the thylakoid Tat translocase during protein transport. J. Biol. Chem. *281*, 5476–5483.

De Keersmaeker, S., Vrancken, K., Van Mellaert, L., Anne, J., and Geukens, N. (2007). The Tat pathway in *Streptomyces lividans*:

interaction of Tat subunits and their role in translocation. Microbiology *153*, 1087–1094.

Frielingsdorf, S. and Klösgen, R.B. (2007). Prerequisites for terminal processing of thylakoidal Tat substrates. J. Biol. Chem. *282*, 24455–24462.

Fröbel, J., Rose, P., Lausberg, F., Blummel, A.S., Freudl, R., and Müller, M. (2012). Transmembrane insertion of twin-arginine signal peptides is driven by TatC and regulated by TatB. Nat. Commun. *3*, 1311.

Gerard, F. and Cline, K. (2006). Efficient twin arginine translocation (Tat) Pathway transport of a precursor protein covalently anchored to its initial cpTatC binding site. J. Biol. Chem. *281*, 6130–6135.

Gerard, F. and Cline, K. (2007). The thylakoid proton gradient promotes an advanced stage of signal peptide binding deep within the Tat pathway receptor complex. J. Biol. Chem. *282*, 5263–5272.

Gogala, M., Becker, T., Beatrix, B., Armache, J.P., Barrio-Garcia, C., Berninghausen, O., and Beckmann, R. (2014). Structures of the Sec61 complex engaged in nascent peptide translocation or membrane insertion. Nature *506*, 107–110.

Goosens, V.J., Monteferrante, C.G., and van Dijl, J.M. (2014). The Tat system of Gram-positive bacteria. Biochim Biophys Acta. *1843*, 1698–1706.

Guex, N. and Peitsch, M.C. (1997). SWISS-MODEL and the Swiss-PdbViewer: an environment for comparative protein modeling. Electrophoresis *18*, 2714–2723.

Halbig, D., Wiegert, T., Blaudeck, N., Freudl, R., and Sprenger, G.A. (1999). The efficient export of NADP-containing glucose-fructose oxidoreductase to the periplasm of *Zymomonas mobilis* depends both on an intact twin-arginine motif in the signal peptide and on the generation of a structural export signal induced by cofactor binding. Eur. J. Biochem. *263*, 543–551.

Hou, B. and Brüser, T. (2011). The Tat-dependent protein translocation pathway. Biomol. Concepts. *2*, 507–523.

Hou, B., Lin, P.J., and Johnson, A.E. (2012). Membrane protein TM segments are retained at the translocon during integration until the nascent chain cues FRET-detected release into bulk lipid. Mol. Cell. *48*, 398–408.

Ize, B., Gerard, F., Zhang, M., Chanal, A., Voulhoux, R., Palmer, T., Filloux, A., and Wu, L.F. (2002). *In vivo* dissection of the Tat translocation pathway in *Escherichia coli*. J. Mol. Biol. *317*, 327–335.

Ize, B., Stanley, N.R., Buchanan, G., and Palmer, T. (2003). Role of the *Escherichia coli* Tat pathway in outer membrane integrity. Mol. Microbiol. *48*, 1183–1193.

Jack, R.L., Sargent, F., Berks, B.C., Sawers, G., and Palmer, T. (2001). Constitutive expression of *Escherichia coli tat* genes indicates an important role for the twin-arginine translocase during aerobic and anaerobic growth. J. Bacteriol. *183*, 1801–1804.

Jakob, M., Kaiser, S., Gutensohn, M., Hanner, P., and Klösgen, R.B. (2009). Tat subunit stoichiometry in Arabidopsis thaliana challenges the proposed function of TatA as the translocation pore. Biochim. Biophys. Acta. *1793*, 388–394.

Kauer, J.C., Erickson-Viitanen, S., Wolfe, H.R. Jr., and DeGrado, W.F. (1986). p-Benzoyl-L-phenylalanine, a new photoreactive amino acid. Photolabeling of calmodulin with a synthetic calmodulin-binding peptide. J. Biol. Chem. *261*, 10695–10700.

Kreutzenbeck, P., Kröger, C., Lausberg, F., Blaudeck, N., Sprenger, G.A., and Freudl, R. (2007). *Escherichia coli* twin arginine (Tat) mutant translocases possessing relaxed signal peptide recognition specificities. J. Biol. Chem. *282*, 7903–7911.

Lausberg, F., Fleckenstein, S., Kreutzenbeck, P., Fröbel, J., Rose, P., Müller, M., and Freudl, R. (2012). Genetic evidence for a tight cooperation of TatB and TatC during productive recognition of twin-arginine (Tat) signal peptides in Escherichia coli. PLoS One *7*, e39867.

Lindenstrauß, U. and Brüser, T. (2009). Tat transport of linker-containing proteins in *Escherichia coli*. FEMS Microbiol. Lett. *295*, 135–140.

Maurer, C., Panahandeh, S., Jungkamp, A.C., Moser, M., and Müller, M. (2010). TatB functions as an oligomeric binding site for folded Tat precursor proteins. Mol. Biol. Cell. *21*, 4151–4161.

Mori, H. and Cline, K. (2002). A twin arginine signal peptide and the pH gradient trigger reversible assembly of the thylakoid ΔpH/Tat translocase. J. Cell Biol. *157*, 205–210.

Oates, J., Barrett, C.M., Barnett, J.P., Byrne, K.G., Bolhuis, A., and Robinson, C. (2005). The *Escherichia coli* twin-arginine translocation apparatus incorporates a distinct form of TatABC complex, spectrum of modular TatA complexes and minor TatAB complex. J. Mol. Biol. *346*, 295–305.

Pal, D., Fite, K., and Dabney-Smith, C. (2013). Direct interaction between a precursor mature domain and transport component Tha4 during twin arginine transport of chloroplasts. Plant Physiol. *161*, 990–1001.

Palmer, T. and Berks, B.C. (2012). The twin-arginine translocation (Tat) protein export pathway. Nat. Rev. Microbiol. *10*, 483–496.

Park, E., Menetret, J.F., Gumbart, J.C., Ludtke, S.J., Li, W., Whynot, A., Rapoport, T.A., and Akey, C.W. (2014). Structure of the SecY channel during initiation of protein translocation. Nature *506*, 102–106.

Pop, O.I., Westermann, M., Volkmer-Engert, R., Schulz, D., Lemke, C., Schreiber, S., Gerlach, R., Wetzker, R., and Müller, J.P. (2003). Sequence-specific binding of prePhoD to soluble TatAd indicates protein-mediated targeting of the Tat export in *Bacillus subtilis*. J. Biol. Chem. *278*, 38428–38436.

Ramasamy, S., Abrol, R., Suloway, C.J., and Clemons, W.M. Jr. (2013). The glove-like structure of the conserved membrane protein TatC provides insight into signal sequence recognition in twin-arginine translocation. Structure *21*, 777–788.

Richter, S. and Brüser, T. (2005). Targeting of unfolded PhoA to the TAT translocon of *Escherichia coli*. J. Biol. Chem. *280*, 42723–42730.

Richter, S., Lindenstrauss, U., Lücke, C., Bayliss, R., and Brüser, T. (2007). Functional Tat transport of unstructured, small, hydrophilic proteins. J. Biol. Chem. *282*, 33257–33264.

Rodriguez, F., Rouse, S.L., Tait, C.E., Harmer, J., De Riso, A., Timmel, C.R., Sansom, M.S., Berks, B.C., and Schnell, J.R. (2013). Structural model for the protein-translocating element of the twin-arginine transport system. Proc. Natl. Acad. Sci. USA *110*, E1092–E1101.

Rollauer, S.E., Tarry, M.J., Graham, J.E., Jaaskelainen, M., Jager, F., Johnson, S., Krehenbrink, M., Liu, S.M., Lukey, M.J., Marcoux, J., et al. (2012). Structure of the TatC core of the twin-arginine protein transport system. Nature *492*, 210–214.

Ryu, Y. and Schultz, P.G. (2006). Efficient incorporation of unnatural amino acids into proteins in *Escherichia coli*. Nat. Met. *3*, 263–265.

Sargent, F., Stanley, N.R., Berks, B.C., and Palmer, T. (1999). Sec-independent protein translocation in *Escherichia coli*. A

distinct and pivotal role for the TatB protein. J. Biol. Chem. *274*, 36073–36082.

Silvestro, A., Pommier, J., Pascal, M.C., and Giordano, G. (1989). The inducible trimethylamine N-oxide reductase of *Escherichia coli* K12: its localization and inducers. Biochim. Biophys. Acta. *999*, 208–216.

Stanley, N.R., Palmer, T., and Berks, B.C. (2000). The twin arginine consensus motif of Tat signal peptides is involved in Sec-independent protein targeting in *Escherichia coli*. J. Biol. Chem. *275*, 11591–11596.

Yen, M.R., Tseng, Y.H., Nguyen, E.H., Wu, L.F., and Saier, M.H., Jr. (2002). Sequence and phylogenetic analyses of the twin-arginine targeting (Tat) protein export system. Arch. Microbiol. *177*, 441–450.

Young, T.S., Ahmad, I., Yin, J.A., and Schultz, P.G. (2010). An enhanced system for unnatural amino acid mutagenesis in *E. coli*. J. Mol. Biol. *395*, 361–374.